A Compact CPW Bandpass Filter Based on Spiral-Shaped DGSs for 5G Frequency Band

Wen Huang[1, *], Lu Li[1], Liang Li[1], and Jinsheng Dong[2]

Abstract—A CPW (coplanar waveguide) bandpass filter based on spiral-shaped DGSs (defected ground structures) which can be used in the 5G band is proposed. Two pairs of face-to-face symmetrical spiral-shaped DGSs are added to the ground planes of a CPW main transmission line. A cross-shaped notch is adopted in the central strip of the CPW main transmission line to generate the passband, while two m-shaped DGSs are brought in to improve the passband performance of the filter. The measured results show that the central frequency is 3.54 GHz, and the 3-dB bandwidth is from 3.29 GHz to 3.79 GHz. The filter has a 10.1% bandwidth with a return loss better than 10 dB from 3.35 GHz to 3.71 GHz, and the insertion loss is less than 2.0 dB in the passband. Besides, there are two transmission zeros near the passband at 2.45 GHz and 4.81 GHz, which can improve the stopband rejection.

1. INTRODUCTION

As one of the key components of wireless communication systems, filters have a very important role in the RF front-end. Especially in the context of the 5G era, the performances of filters are increasingly demanded. Stepped-impedance resonator (SIR) [1] and stub-loaded resonator (SLR) [2] are introduced for filters to achieve wide stopband, but with relatively large circuit sizes. To improve the passband and stopband performance with circuit miniaturization, the filters based on a slow-wave resonator are proposed [3]. However, realizing bandpass filters with low insertion losses and compact structures remains a great challenge.

CPW transmission line has a good dispersive property, and it can realize a broadband effect in circuits [4]. With the rapid development of 5G communication technology, communication systems not only need to improve the transmission rate but also require wider bandwidth than before, so CPW filter plays an essential role in the RF front-end.

So far, different bandpass filters have been realized with CPW structures [5–7]. In [5], high selective bandpass filters using end-connected conductor-backed coplanar waveguide are designed, but the double-layer circuit is not convenient for the connection between components. In [6], the proposed bandpass filter is based on slow-wave CPW resonators designed by conventional and tapered CPW sections with short-stub. The two resonators are connected back-to-back to realize the passband and improve the stopband rejection. In [7], a compact bandpass filter with spiral-shaped DGSs is proposed, adopting an interdigital structure and T-shaped patches in the central strip of the CPW main transmission line. Besides the CPW circuit, passband filters with other circuit forms using spiral-shaped DGSs have been reported [8–10]. In [8], a microstrip bandpass filter with two symmetrical spiral-shaped DGSs is presented, and the passband insertion loss is large. In [9], the bandpass filter is designed with a silicon substrate integrated passive device technology, which utilizes spiral DGSs and interdigital structure. This filter has greatly reduced the physical size, but the insertion loss is relatively large with 4.8 dB

minimum insertion loss. In [10], a bandpass filter is proposed with spiral-shaped DGSs using a microstrip circuit. However, this structure is designed on both sides of the substrate and not easy to connect with other components.

In this paper, a CPW bandpass filter based on spiral-shaped DGSs and m-DGSs is proposed for the 5G frequency band. The four spiral-shaped DGSs located in the ground planes of the CPW main transmission line make the out-of-band suppression ideal and realize miniaturization of the filter. Then, the m-DGSs are brought in to improve the passband performance of the filter. Compared with other filters using spiral-shaped DGSs, the proposed filter is simple to fabricate and easy to integrate with other circuits while it keeps excellent passband performance.

2. ANALYSIS OF THE SPIRAL-SHAPED DGSS

As shown in Figure 1(a), a section of spiral-shaped DGSs is composed of two spiral-shaped DGSs in each ground plane of the CPW main transmission line, where the metal part and etched part are represented by gray and white colors, respectively. The length and width of spiral-shaped DGS is denoted by a, and the gap and width of the spiral strip are b_1 and b_2, respectively. The equivalent circuit of the spiral-shaped DGSs is illustrated in Figure 1(b). The central strip and gaps of the CPW can be equivalent to series inductor L_1 and shunt capacitors C_1. Each spiral-shaped DGS can be equivalent to an LC parallel resonant circuit composed of a capacitor C_s and an inductor L_s.
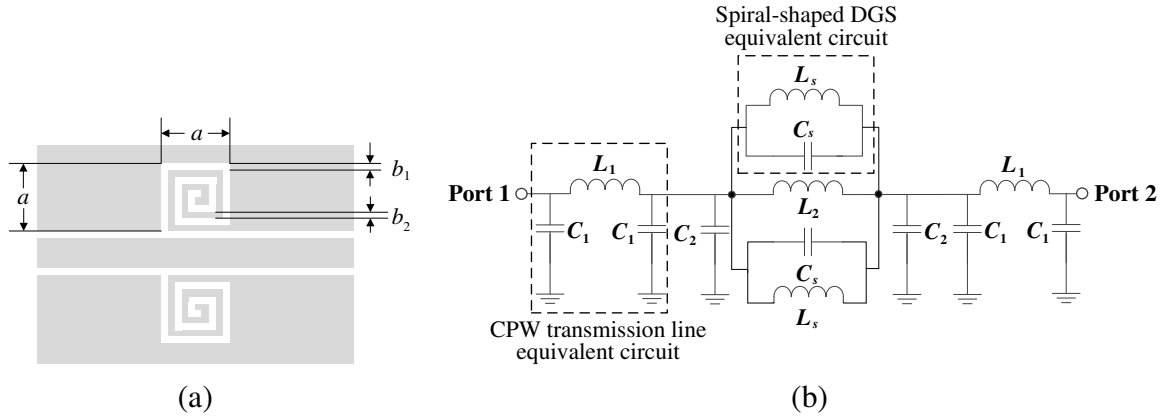

Figure 1. A section of spiral-shaped DGSs. (a) Layout. (b) Equivalent circuit.

The spiral-shaped DGS is designed to have the same filtering performance as a one-pole Butterworth lowpass filter. Then the equivalent circuit element parameters L_s and C_s in the equivalent circuit of the spiral-shaped DGS can be calculated, when the spiral-shaped DGS is satisfied with the same attenuation conditions as the one-pole Butterworth lowpass filter. As shown in Figure 1(b), the impedance of the LC parallel resonant circuit corresponding to the spiral-shaped DGS can be expressed as

$$Z_{LC} = jX_{LC} = j\omega L_s // \frac{1}{j\omega C_s} = j\frac{\omega}{C_s\left(\omega_0^2 - \omega^2\right)} \tag{1}$$

where ω_0 is the resonant angular frequency of the LC parallel resonant circuit corresponding to the spiral-shaped DGS. Figure 2 shows the equivalent circuit of the one-pole Butterworth lowpass filter [11], where the impedances of both ports are $50\,\Omega$. The impedance of the series inductor of the one-pole Butterworth lowpass filter can be obtained as

$$Z_L = jX_L = \frac{j\omega Z_0 g_1}{\omega_c} \tag{2}$$

where g_1 is a prototype value of the Butterworth lowpass filter, and the value is 2. ω_c is the 3-dB cut-off angular frequency, and Z_0 is the characteristic impedance of input and output ports.
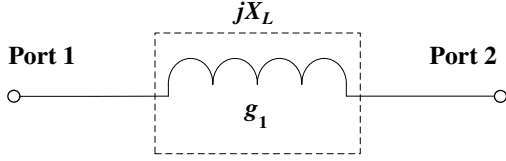
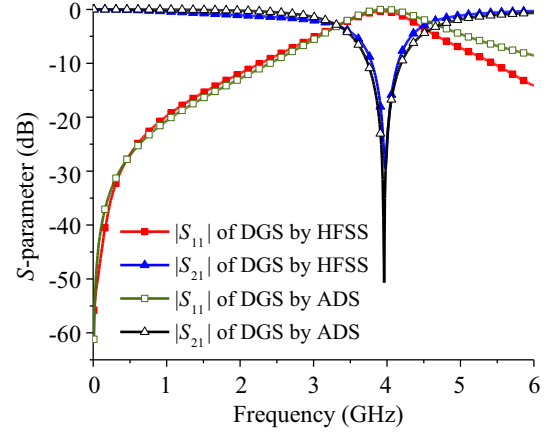**Figure 2.** Equivalent circuit of one-pole Butterworth lowpass filter.

Figure 3. Simulations of the spiral-shaped DGS.

The LC parallel resonant circuit of the spiral-shaped DGS is designed to have the same cut-off frequency and attenuation characteristics with a one-pole Butterworth lowpass filter. So, at a certain angular frequency $\omega = \omega_c$, the impedance of the Butterworth lowpass filter and the LC parallel resonant circuit corresponding to the spiral-shaped DGS should be equal, then the equation can be given by

$$Z_{LC}|_{\omega=\omega_c} = Z_L|_{\omega=\omega_c} \tag{3}$$

From the above equations, the equivalent capacitance C_s and inductance L_s of the spiral-shaped DGS can be obtained as

$$C_s = \frac{\omega_c}{Z_0 g_1 \left(\omega_0^2 - \omega_c^2\right)} = \frac{f_c}{4\pi Z_0 \left(f_0^2 - f_c^2\right)} \tag{4}$$

$$L_s = \frac{1}{\omega_0^2 C_s} = \frac{1}{4\pi^2 f_0^2 C_s} \tag{5}$$

The simulated s-parameters of the spiral-shaped DGS are displayed in Figure 3. It can be seen from Figure 3 that the 3-dB cut-off frequency f_c of spiral-shaped DGS is 3.32 GHz, and the resonant frequency f_0 is 3.96 GHz. Then, the equivalent circuit parameters of the spiral-shaped DGS can be obtained according to Equations (4) and (5). The calculated equivalent element parameters are $L_s = 1.39$ nH, $C_s = 1.16$ pF. With the dimensions of $a = 3.0$ mm, $b_1 = 0.3$ mm, $b_2 = 0.3$ mm, the layout of spiral-shaped DGS has been simulated by the electromagnetics simulation solver of HFSS, while the equivalent lumped circuit has been simulated by the software of ADS, as shown in Figure 3. The agreements between them demonstrate the validity of equivalent circuit parameters extraction.

3. DESIGN OF THE SPIRAL-SHAPED DGSS BANDPASS FILTER

Based on the spiral-shaped DGSs, a bandpass filter is designed, as shown in Figure 4(a). The bandpass filter consists of a CPW transmission line with a cross-shaped notch located at the central strip and two pairs of face-to-face symmetrical spiral-shaped DGSs. The spiral-shaped DGSs can offer the lowpass characteristic with one finite transmission-zero at the upper frequency for the passband filter. The cross-shaped notch makes the central strip line of the CPW main transmission line end-coupled, which can impose another transmission-zero at the lower-frequency. So, they offer bandpass characteristic bounded with two finite transmission-zeros. The two transmission-zeros can be varied by the sizes of spiral-shaped DGSs and the width of the cross-shaped notch. Moreover, the m-shaped DGSs are introduced on each ground plane of the CPW main transmission line to improve the passband performance of the filter, as shown in Figure 4(b). Figure 5 exhibits the whole equivalent circuit of the proposed bandpass filter with spiral-shaped DGSs and m-shaped DGSs. The cross-shaped notch works as the series capacitor C_0. The added m-shaped DGSs introduce the equivalent capacitor C_3 and inductors L_4.
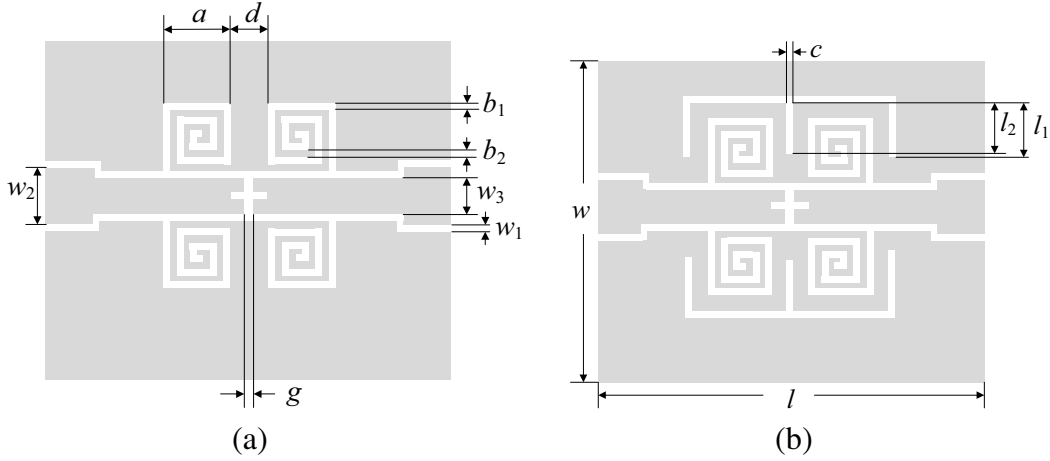
Figure 4. Layouts of bandpass filters. (a) Without m-shaped DGSs. (b) With m-shaped DGSs.
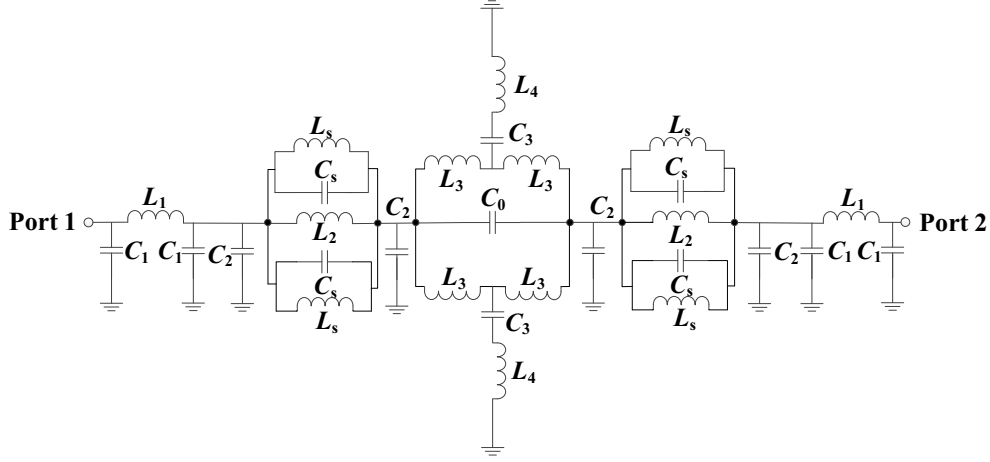

Figure 5. Equivalent circuit of the proposed bandpass filter with spiral-shaped DGSs and m-shaped DGSs.

An example of the proposed bandpass filter, with the DGS dimensions of $a = 3.0$ mm, $b_1 = 0.3$ mm, $b_2 = 0.3$ mm, $d = 2.0$ mm, $c = 0.2$ mm, $l_1 = 3.2$ mm, $l_2 = 2.2$ mm, the $50\,\Omega$ main transmission line dimensions of $w_1 = 0.2$ mm, $w_2 = 3$ mm, $w_3 = 1.2$ mm, the cross-shaped notch width $g = 1.2$ mm, and the circuit size of $w = 25$ mm, $l = 28$ mm, has been simulated with HFSS. Considering the bandpass characteristics are kept, three key dimensions including the length and width a of spiral-shaped DGS, the distances d between two spiral-shaped DGSs, the cross-shaped notch width g, which can significantly affect the central frequency, bandwidth, and also the transmission-zero frequencies, are investigated as follows.

The central frequency of the proposed CPW bandpass filter is mainly determined by the sizes of the spiral-shaped DGSs. With different lengths and widths a of the spiral-shaped DGS, the simulated s-parameters of the proposed filter are shown in Figure 6. It can be seen from Figure 6 that the central frequency is decreased when the length and width a is increased. Meanwhile, with the increased length and width a, both of the lower and upper transmission-zero frequencies are decreased. So, when $a = 3.1$ mm, the central frequency of the filter is close to 3.5 GHz, and the two transmission zeros can be relatively close to the passband.

The simulated s-parameters with different distances d between two spiral-shaped DGSs are shown in Figure 7, and it is stated that the lower transmission-zero frequency is decreased slightly as the distance d is increased, while the upper transmission zero near 4.8 GHz is almost unchanged. With the
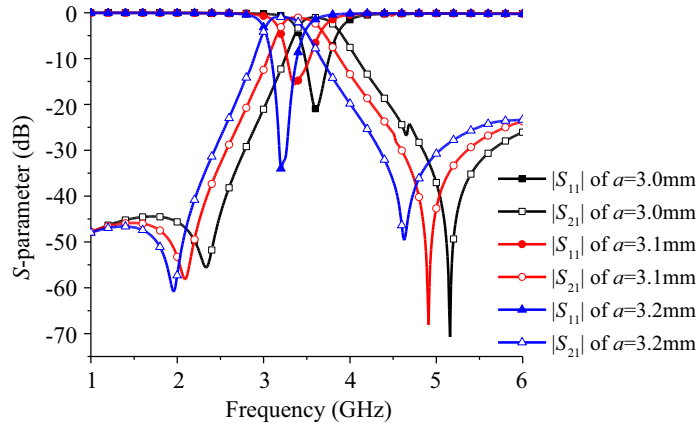
Figure 6. Simulated s-parameters of the proposed filter with different length and width a ($d = 2$ mm, $g = 1.2$ mm).
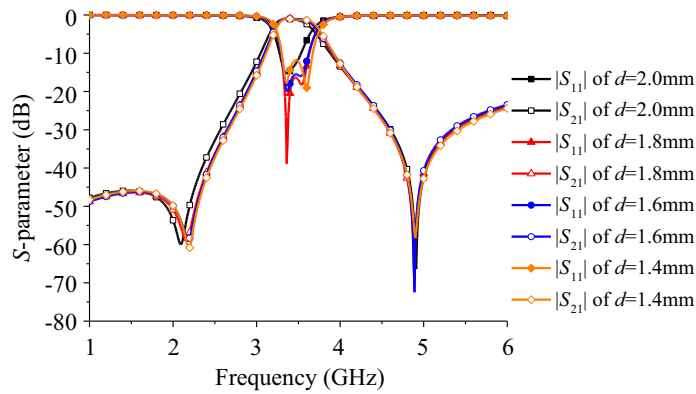

Figure 7. Simulated s-parameters of the proposed filter with the difference width d ($a = 3.1$ mm, $g = 1.2$ mm).

increased distance d, the passband width is also changed. When $d = 1.8$ mm, the overall performance of the filter is good.

The frequencies of the transmission zeros can be tuned not only by the length and width a of the spiral-shaped DGS, but also by the width of the cross-shaped notch, and the simulated results are shown in Figure 8. It can be seen from Figure 8 that when the notch width g is increased from 0.4 mm to 1.6 mm, the lower transmission-zero frequency is decreased from 2.65 GHz to 1.87 GHz, while the upper transmission-zero frequency is increased from 4.75 GHz to 5.18 GHz. However, when the notch width g is increased to more than 2 mm, the lower transmission-zero frequency is still decreased to a lower frequency, while the upper transmission-zero frequency is also decreased slightly to a lower frequency. So, the notch width g is chosen to 0.4 mm to make sure the two transmission zeros near the passband as close as possible.

The simulated performance comparisons of bandpass filters without and with m-shaped DGSs are illustrated in Figure 9. For each filter, the central frequencies are 3.5 GHz, and there are two transmission zeros outside the passband. The bandpass filter with m-shaped DGSs has a return loss of 28.8 dB at 3.5 GHz, while the one without m-DGSs has a return loss of 8.9 dB at 3.5 GHz. The added m-DGSs can increase the 3-dB fractional bandwidth at 3.5 GHz from 5.43% to 12% and decrease the insertion loss at the central frequency from 2.1 dB to 1.07 dB. It can be proved that m-shaped DGSs can improve the passband performance. To weld the SMA connectors conveniently, the port width w_2 is designed wider than the central strip width w_3 of the CPW main transmission line. As the notations marked in Figure 4, the final optimized sizes of the bandpass filter are $w = 25$ mm, $l = 28$ mm, $w_1 = 0.2$ mm,
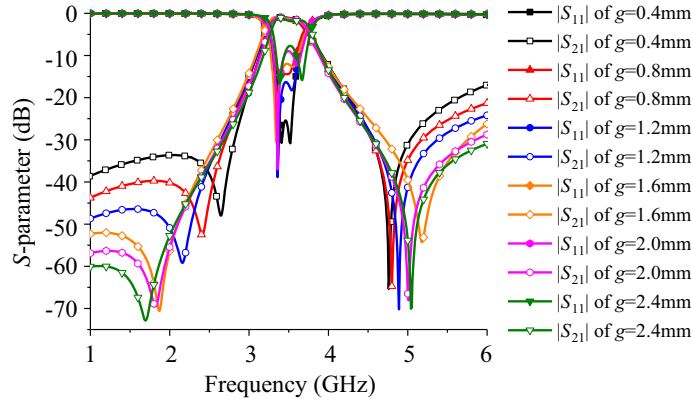
Figure 8. Simulated transmission zeros with different cross-shaped notch width g ($a = 3.1$ mm, $d = 1.8$ mm).
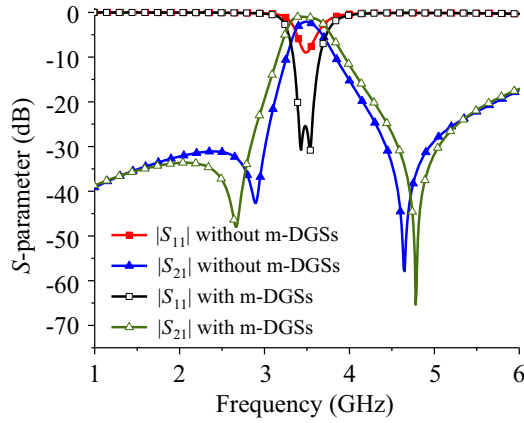

Figure 9. Simulated s-parameters of the filter with m-shaped DGSs and without m-shaped DGSs.

$w_2 = 3$ mm, $w_3 = 1.2$ mm, $g = 0.4$ mm, $d = 1.8$ mm, $a = 3.1$ mm, $b_1 = 0.3$ mm, $b_2 = 0.3$ mm, $l_1 = 3.2$ mm, $l_2 = 2.2$ mm, $c = 0.2$ mm.

e simulated performance comparisons of bandpass filters without and with m-shaped DGSs are illustrated in Figure 9. For each filter, the central frequencies are 3.5 GHz and there are two transmission zeros outside the passband. The bandpass filter with m-shaped DGSs has a return loss of 28.8 dB at 3.5 GHz, while the one without m-DGSs has a return loss of 8.9 dB at 3.5 GHz.

4. FABRICATION AND MEASURED RESULTS

All of the layout simulations are performed by a full-wave simulation software of HFSS. The proposed filter is fabricated on an F4B substrate with 1 mm thickness, relative permittivity $\varepsilon_r = 2.65$, loss tangent $\delta = 0.005$, and the size is 28.0 mm × 25.0 mm. Measurements are carried out by Agilent 8510C network analyzer. A photograph of the fabricated filter is shown in Figure 10.

Figure 11 gives the simulated and measured results of the proposed filter. For simulations, the central frequency is 3.5 GHz while measurements exhibit that the central frequency is 3.54 GHz. There exists a frequency deviation of 0.04 GHz for central frequency due to fabrication tolerance and measurement devices. The measured 3-dB bandwidth is 0.5 GHz from 3.29 GHz to 3.79 GHz. The filter has a 10.1% bandwidth with a return loss better than 10 dB from 3.35 GHz to 3.71 GHz, and the insertion loss is less than 2.0 dB in the passband. Besides, there are two transmission zeros near the passband at 2.45 GHz and 4.81 GHz, with 34.0 dB and 44.0 dB attenuations, respectively, which can improve the stopband rejection. The lower stopband rejection is better than 20 dB from 1.0 GHz to
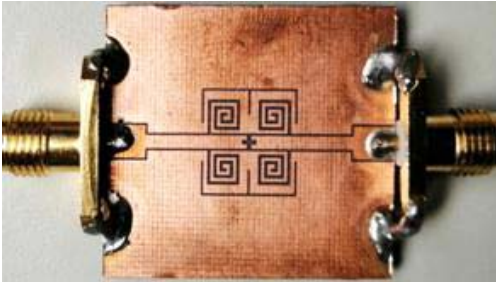
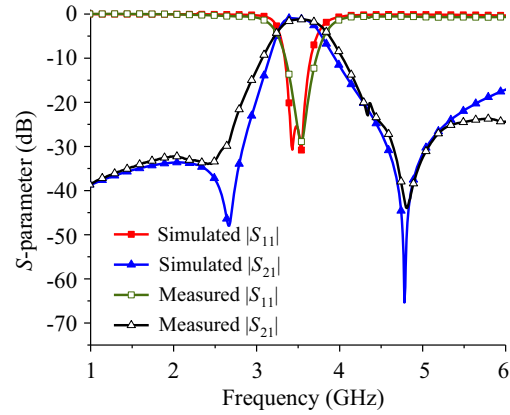**Figure 10.** Photograph of the fabricated bandpass filter.

Figure 11. Simulated and measured s-parameters of the proposed bandpass filter.

2.82 GHz, and the upper stopband rejection is also better than 20 dB from 4.29 GHz up to 7 GHz. The measurements agree well with the simulations.

Table 1 gives performance comparisons of the proposed bandpass filter with some reported bandpass filters, where RL and IL represent the return loss and insertions loss, respectively. $\text{FBW}_{10\,\text{dB}}$ represents the 10-dB fractional bandwidth at the central frequency, f_{TZ} the transmission-zero frequency, and λ_g the guided wavelength at central frequency. The comparisons show that the proposed bandpass filter has a good performance.

Table 1. Performance comparisons of bandpass filters.

	f_0 (GHz)	at f_0		Passband IL (dB)	$\text{FBW}_{10\,\text{dB}}$	f_{TZ} (GHz)	Size
		RL (dB)	IL (dB)				
[4]	6.0	15.3	0.8	< 0.9	66%	3.6/8.9	$0.64\lambda_g \times 0.46\lambda_g$
[5]	3.5	24	1.7	< 2.0	8%	3.0/4.2	$0.37\lambda_g \times 0.31\lambda_g$
[6]	2.16	18	0.9	< 1.1	6.9%	1.5/3.1	$0.19\lambda_g \times 0.65\lambda_g$
[12]	2.35	21	1.3	< 1.5	9.8%	0.79/1.97/2.68/4.11	$0.38\lambda_g \times 0.58\lambda_g$
This work	3.54	28.9	1.23	< 2.0	10.1%	2.45/4.81	$0.42\lambda_g \times 0.37\lambda_g$

5. CONCLUSIONS

In this paper, a CPW bandpass filter using spiral-shaped DGSs and m-shaped DGSs is presented. The two pairs of face-to-face spiral-shaped DGSs and the cross-shaped notch can generate two transmission zeros near the passband. The added m-DGSs can improve the passband performance. From the measurements, the proposed filter is centered at 3.54 GHz with the 10.1% 10-dB fractional bandwidth from 3.35 GHz to 3.71 GHz, and insertion loss is less than 2.0 dB in the passband. Besides, there are two transmission zeros at 2.45 GHz and 4.81 GHz, with 34.0 dB and 44.0 dB attenuation, respectively. The proposed bandpass filter has a good stopband rejection, a compact structure, an easy design and manufacture, and is convenient to connect with other components.

REFERENCES

1. Firmansyah, T., S. Praptodinoyo, R. Wiryadinata, et al., "Dual-wideband bandpass filter using folded cross-stub stepped impedance resonator," *Microw. Opt. Technol. Lett.*, Vol. 59, No. 11, 2929–2934, 2017.

2. Lin, L., B. Wu, T. Su, et al., "Design of tri-band bandpass filter using novel hexa-mode stub-loaded ring resonator," *Microw. Opt. Technol. Lett.*, Vol. 57, No. 9, 2005–2008, 2015.

3. Qin, W., J. Cai, Y. Li, and J. Chen, "Wideband tunable bandpass filter using optimized varactor-loaded SIRs," *IEEE Microw. Wirel. Compon. Lett.*, Vol. 27, No. 9, 812–814, 2017.

4. Gholipour, V., S. M. M. Moshiri, A. Alighanbari, and A. Yahaghi, "Highly selective wideband bandpass filter using combined microstrip/coplanar waveguide structure," *Electronics Letters*, Vol. 52, No. 13, 1145–1147, 2016.

5. Xiao, J., M. Zhu, J. Ma, and J. Hong, "Conductor-backed CPW bandpass filters with electromagnetic couplings," *IEEE Microw. Wirel. Compon. Lett.*, Vol. 26, No. 6, 401–403, 2016.

6. Yang, B., H. J. Qian, Y. Shu, and X. Luo, "Compact bandpass filter with wide stopband using slow-wave CPW resonator with back-to-back coupled-scheme," *IEEE International Symposium on Radio-Frequency Integration Technology (RFIT)*, 13–15, Seoul, South Korea, 2017.

7. Chen, Z., et al., "A high efficiency band-pass filter based on CPW and quasi-spoof surface plasmon polaritons," *IEEE Access*, Vol. 8, 4311–4317, 2020.

8. Letavin, D. A. and V. A. Chechetkin, "Miniature microwave bandpass filter with two circular spiral resonators," *International Conference on Advances in Computing, Communications and Informatics (ICACCI)*, 2315–2317, Jaipur, 2016.

9. Chang, Y.-C., P.-Y. Wang, S. S. H. Hsu, et al., "A V-band CPW bandpass filter with controllable transmission zeros in integrated passive devices (IPD) technology," *IEEE MTT-S International Microwave Symposium*, 1–3, San Francisco, CA, 2016.

10. Peng, B., et al., "Compact quad-mode bandpass filter based on quad-mode DGS resonator," *IEEE Microw. Wirel. Compon. Lett.*, Vol. 26, No. 4, 234–236, 2016.

11. Ahn, D., J. S. Park, C. S. Kim, et al., "A design of the low-pass filter using the novel microstrip defected ground structure," *IEEE Trans. Microwave Theory Tech.*, Vol. 49, No. 1, 86–93, 2001.

12. Xiao, J.-K., X. Qi, H. Wang, and J. Ma, "High selective balanced bandpass filters using end-connected conductor-backed coplanar waveguide," *IEEE Access*, Vol. 7, 16184–16193, 2019.